

# Novel Double Phase Transforming Organogel Based on $\beta$ -Cyclodextrin in 1,2-Propylene Glycol

Wenqi Liu, Pengyao Xing, Feifei Xin, Yuehui Hou, Tao Sun, Jingcheng Hao, and Aiyou Hao\*

Key Laboratory of Colloid and Interface Chemistry (Shandong University), Ministry of Education, Jinan 250100, P. R. China

**S** Supporting Information



**ABSTRACT:** This paper describes a novel double phase transforming organogel (gel–sol–gel') composed of nontoxic  $\beta$ -cyclodextrin, potassium carbonate, and 1,2-propylene glycol. The gel–sol–gel' transforming processes are followed by a reversible gel–sol transforming process and an irreversible sol–gel' transforming process based on heating. The gel–sol–gel' transformation is accompanied by microstructure changes from nanospheres to nanorods.  $K_2CO_3$  plays a key role in associating supramolecular architectures of  $\beta$ -cyclodextrin into a three-dimensional network. This work may bring further applications in the areas of smart materials, drug delivery systems, and biomaterials.

## 1. INTRODUCTION

In recent years, expanding novel stimuli-responsive functional materials is becoming highly desirable,<sup>1–4</sup> and the organogels based on supramolecular interactions are definitely valuable commodities for their versatile applications in drug delivery systems,<sup>5,6</sup> templates for preparing inorganic and hybrid nanofibrous materials,<sup>7</sup> molecular electronics,<sup>8</sup> sensors,<sup>9</sup> and so forth.<sup>10–12</sup> The formation of organogels based on supramolecular structures arises from noncovalent interactions like H-bonding,  $\pi$ – $\pi$  stacking, donor–acceptor interactions, metal coordination, van der Waals interactions, and other weak interactions.<sup>13–15</sup> These interactions can induce the formation of supramolecular architectures with various morphologies like fibers,<sup>16</sup> rods,<sup>17</sup> ribbons,<sup>18</sup> and cubes.<sup>19,20</sup> These supramolecular architectures could aggregate further via junction zones to form 3D networks which immobilize the solvent through interface tension and capillary forces.<sup>20,21</sup>

The general organogels are sol–gel systems, which are prepared by introducing the stimuli factors like light,<sup>22</sup> heat,<sup>23</sup> ultrasonic,<sup>24</sup> etc., to a solution or pregel colloidal suspension.<sup>11</sup> The stimuli-responsive properties of these systems are the key factors to be considered as the functional materials. Designing novel stimuli-responsive gelation systems based on morphologic changing induced by external stimuli might bring further applications.<sup>25,26</sup>

Here we report a novel stimuli-responsive organogel system prepared by  $\beta$ -cyclodextrin ( $\beta$ -CD),  $K_2CO_3$  in 1,2-propylene glycol. This is a double phase transforming (gel–sol–gel') organogel system, and the transforming processes are followed by a reversible gel–sol transforming process and an irreversible sol–gel' transforming process based on heating. According to our best knowledge, such kind of unique behaviors of the gel–

sol–gel' transforming is first reported in this paper. The gel–sol–gel' transformation is accompanied by microstructure changes from nanospheres composed of shorter channel-type  $\beta$ -CD assemblies to nanorods which are composed of longer channel-type  $\beta$ -CD assemblies.  $K_2CO_3$  plays a key role in associating supramolecular architectures of  $\beta$ -CD. The gel system is a nontoxic system, which could be expected to be used in body-friendly smart materials, drug-delivery systems, and biomaterials.

## 2. EXPERIMENTAL SECTION

**2.1. Chemicals and Materials.**  $\beta$ -CD purchased from Zhi Yuan Group Fine Chemical Co., Ltd., was recrystallized three times in distilled water.  $K_2CO_3$  was purchased from Tian Jin Ke Meng Chemical Industry and Trade Co., Ltd., and was used without further purification. 1,2-Propylene glycol was purchased from Tian Jin Kermel Reagent Co., Ltd., and was used without further purification. Other materials were used as received.

**2.2. Preparation of the Gels.** A mixture of  $\beta$ -CD and  $K_2CO_3$  in an appropriate ratio was added into the solvent of 1,2-propylene glycol. The sample was heated under stirring in the oil bath at 100 °C until the solution was homogeneous. Gel A was formed upon self-cooling the sample to 25 °C. After heating gel A to the gel–sol transition temperature ( $T_{GS}$ ), the homogeneous solution reappeared. Gel B was formed upon heating the homogeneous solution to the sol–gel' transition temperature ( $T_{SG'}$ ).

Received: June 30, 2012

Revised: September 30, 2012

Published: October 10, 2012



**Figure 1.** Photographs of the gel–sol–gel' transition process: (a) gel A formed after cooling the solution; (b) homogeneous solution obtained after heating gel A; (c) gel B formed after heating the solution.

**2.3. Measurement of  $T_{GS}$  and  $T_{SG}$ .** We used the method of tube inversion for gelation characterization.<sup>23</sup> A tube containing gel A was immersed in a temperature-controlled oil bath. The temperature at which the sample started to flow was recorded as  $T_{GS}$ . The temperature at which the solution showed no fluidity and did not fall down after heating the solution was recorded as  $T_{SG}$ .

**2.4. Scanning Electron Microscopy (SEM) Measurements.** Xerogel A sample was prepared by drying gel A at 25 °C for 10 days under a high vacuum while xerogel B sample was obtained at 100 °C for 6 h. SEM images of the xerogels were obtained using a Hitachi S-4800 scanning electron microscope after coating the xerogels with gold.

**2.5. Differential Scanning Calorimetry (DSC) Measurements.** A DSC822<sup>e</sup> thermal analysis system from Mettler-Toledo (Swiss) was employed. The gel sample (between 5 and 15 mg) was weighed into unsealed aluminum pans. The DSC thermogram was recorded with the temperature ranging from 25 to 140 °C at the heating rate of 5 °C min<sup>−1</sup> under a N<sub>2</sub> atmosphere with the reference of empty aluminum.

**2.6. Rheology.** Rheological properties were measured by a Thermo Haake RS300 rheometer with cone and plate geometry (35 mm diameter, 0.105 mm cone gap). The frequency spectra were conducted in the linear viscoelastic regime of the samples determined from dynamic strain sweep measurements at 25 °C.

**2.7. Small-Angle XRD Measurements.** The X-ray diffraction (XRD) patterns were recorded using a Rigaku D/Max 2200-PC diffractometer with Cu K $\alpha$  radiation ( $\lambda = 0.154$  18 nm) and a graphite monochromator at ambient temperature. The samples were tested from 5° to 20° at the scanning rate of 1° min<sup>−1</sup>.

**2.8. FT-IR Measurements.** The xerogel samples and native  $\beta$ -CD were measured by a Bruker TENSOR 27 infrared spectrophotometer with a KBr pellet technique within the 4000–500 cm<sup>−1</sup> region.

**2.9. <sup>1</sup>H NMR Measurements.** <sup>1</sup>H NMR spectra of xerogel samples and native  $\beta$ -CD were recorded on a Bruker AVANCE-400 NMR spectrometer at 298 K with D<sub>2</sub>O as the solvent.

**2.10. Molecular Dynamic Simulations.** The dynamic simulations of gel A and gel B were performed with the software Material Studio 4.3 by Accelrys. A compass force was employed in both of the simulations. Both of the models were first energy minimized, and then the 500 ps dynamic simulations were executed with the time step 1 fs. The simulation of gel A was performed at 298 K while gel B was executed at 393 K. Both of the models were performed within the canonical NVT ensemble, and geometries were saved every 5000 steps.

### 3. RESULTS AND DISCUSSION

#### 3.1. Characterization of Gel–Sol–Gel' Transition.

**3.1.1. Gel–Sol–Gel' Transition Process from Gel A to Gel B.** The photograph of the gel–sol–gel' transition process is

shown in Figure 1. Gel A (Figure 1a) was formed after self-cooling the homogeneous solution (Figure 1b) to 25 °C. The solution reappeared upon heating gel A to  $T_{GS}$ . The reversible process could be repeated several times without changing the properties of the system. Gel B (Figure 1c) was formed after heating the homogeneous solution to  $T_{SG}$ . Interestingly, when the concentration of  $\beta$ -CD was lower than 0.088 mol L<sup>−1</sup>, gel B showed an exceptional thermal stability. It could be heated to the boiling point of the solvent (188 °C) without changing its morphologies. Gel B could not come back to the solution after cooling the temperature to 25 °C.

**3.1.2. Microstructure Transition from Gel A to Gel B.** To further investigate the morphologies of the gel system, xerogel samples of gel A and gel B were observed by SEM. As shown in Figure 2a, the microstructure of gel A was an accumulation of

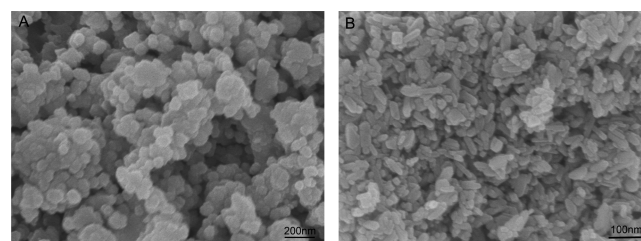


**Figure 2.** SEM images of xerogels of gel A (A) and xerogels of gel B (B).

sphere-like microparticles with the diameter about 100 nm. In contrast, the microstructure of gel B (Figure 2b) presented an accumulation of more compacted nanorods with the length about 100 nm. From the result we could speculate that the gel–sol–gel' transition process was related to the changes of the microstructure triggered by heating. The  $\beta$ -CD was dispersed in the solution at  $T_{GS}$ . The dispersed  $\beta$ -CD accumulated into nanospheres after cooling the solution, the huge interface tension of the network composed of nanospheres immobilized the solvent, and gel A was observed. The nanospheres were dispersed into the solution again upon heating. When the solution was heated to  $T_{SG}$ , the dispersed  $\beta$ -CD aggregated into nanorods. The capillary forces which immobilized the solvent were formed after the nanorods aggregating further, and gel B was obtained. The closely compacted nanorods could not be dissolved into the solution after cooling; therefore, gel B could not come back to the solution.

**3.1.3. Gel–Sol–Gel' Transition Measured by DSC.** The gel–sol–gel' transition process was further characterized by DSC. As is shown in Figure 3, the two peaks at 81.9 and 109.2 °C were in accordance with the gelation temperature ( $T_{GS}$  and  $T_{SG}$ , respectively). The gel–sol transition was accompanied by an exothermic process from 34.4 to 81.9 °C while the sol–gel' transition was accompanied by an endothermic process from 81.9 to 109.2 °C. When the temperature was over 109.2 °C, the

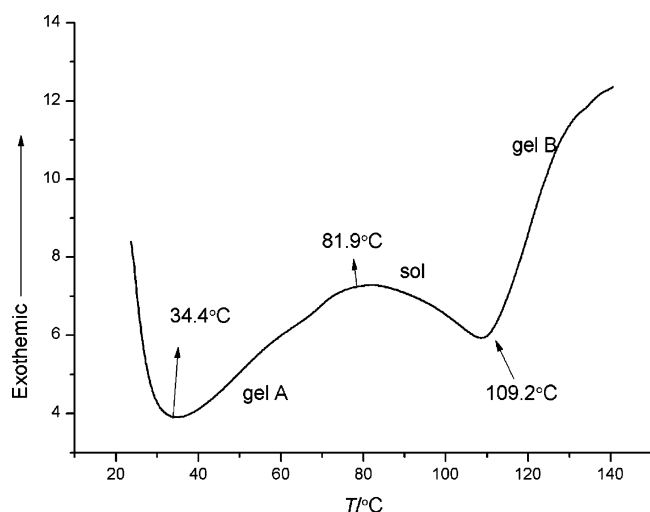


**Figure 3.** Thermal behaviors of the gel-sol-gel' system ( $c_{\beta\text{-CD}} = 0.18 \text{ mol L}^{-1}$ ,  $\omega_{\text{K}_2\text{CO}_3} = 7.3\%$ ,  $\text{K}_2\text{CO}_3/1,2\text{-propylene glycol}$ , w/w).

structure of gel B began to be destroyed, and the process showed an exothermic property.

**3.2. Properties of the Gel-Sol-Gel' Systems.** **3.2.1. Effect of the Concentration of  $\beta\text{-CD}$  on  $T_{\text{GS}}$  and  $T_{\text{SG}}$ .** The concentration of  $\beta\text{-CD}$  could influence the gel-sol-gel' behaviors by changing  $T_{\text{GS}}$  and  $T_{\text{SG}}$ . As shown in Figure 4,

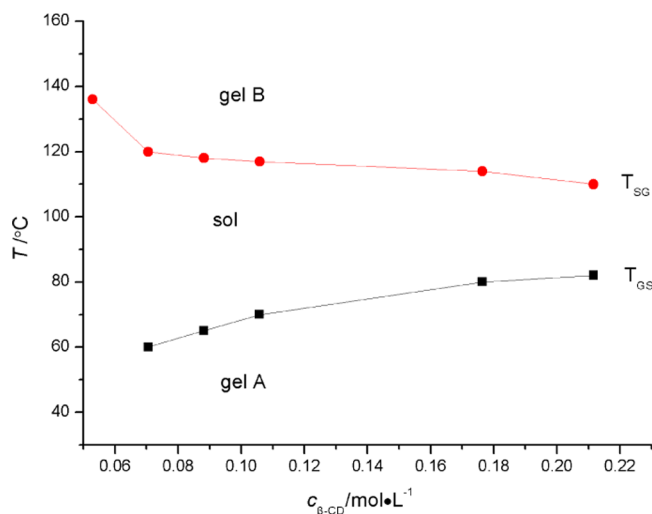


**Figure 4.** Effect of the concentration of  $\beta\text{-CD}$  on  $T_{\text{SG}}$  and  $T_{\text{GS}}$  ( $\omega_{\text{K}_2\text{CO}_3} = 7.3\%$ ,  $\text{K}_2\text{CO}_3/1,2\text{-propylene glycol}$ , w/w).

$T_{\text{GS}}$  could be raised while  $T_{\text{SG}}$  could be reduced with the increase in  $\beta\text{-CD}$  concentration. This result might be related to the formation of denser network of gel A with more concentrated  $\beta\text{-CD}$ , and higher  $T_{\text{SG}}$  was needed to dissolve the denser network. Meanwhile, more concentrated  $\beta\text{-CD}$  solution was easier to form the network for gelating the solution based on heating; thus, lower  $T_{\text{GS}}$  was observed. The minimum gelator concentration (MGC) of gel A is  $0.07 \text{ mol L}^{-1}$  while the MGC of gel B is  $0.05 \text{ mol L}^{-1}$ . This result indicates the nanorods could better gelate the solution. In addition, after substituting  $\beta\text{-CD}$  by  $\alpha\text{-CD}$  or  $\gamma\text{-CD}$ , no gelation behavior was observed.

**3.2.2. Effect of the Concentration of  $\text{K}_2\text{CO}_3$  on  $T_{\text{GS}}$  and  $T_{\text{SG}}$ .** The effect of the concentration of  $\text{K}_2\text{CO}_3$  on  $T_{\text{GS}}$  and  $T_{\text{SG}}$  is

shown in Figure 5. Both  $T_{\text{SG}}$  and  $T_{\text{SG}}$  could be raised with the increased concentration. According to the result, it could be

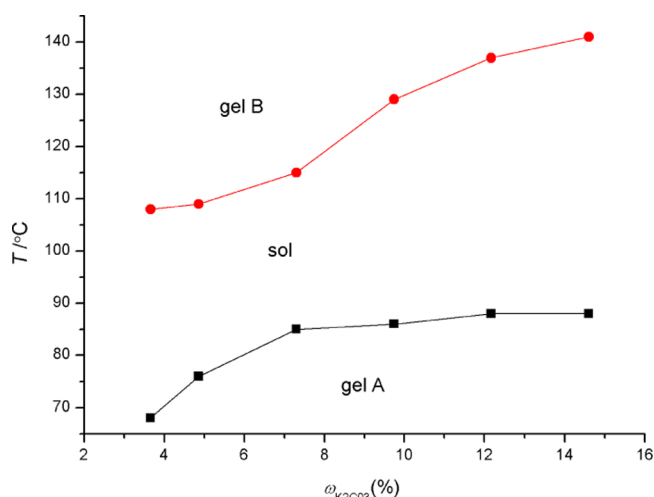


**Figure 5.** Effect of the concentration of  $\text{K}_2\text{CO}_3$  on  $T_{\text{SG}}$  and  $T_{\text{GS}}$  ( $c_{\beta\text{-CD}} = 0.18 \text{ mol L}^{-1}$ ,  $\omega_{\text{K}_2\text{CO}_3}$ :  $\text{K}_2\text{CO}_3/1,2\text{-propylene glycol}$ , w/w).

speculated that the formations of the gels were related to the concentration of  $\text{K}_2\text{CO}_3$ . More concentrated  $\text{K}_2\text{CO}_3$  could stabilize gel A, maybe by adding more junction zones; therefore, higher temperature was needed to break those junction zones. Meanwhile, more concentrated  $\text{K}_2\text{CO}_3$  could prevent the formation of gel B, probably because more concentrated  $\text{K}_2\text{CO}_3$  led to stronger electrostatic repulsion, and then the orderly aggregation of  $\beta\text{-CD}$ , which was related to the atomic radius and electrical properties of  $\text{K}^+$  and  $\text{CO}_3^{2-}$ , became harder.

**3.2.3. Effect of the Salt on the Gelation.** Detailed experimental observations of the influence of the salts on gelation indicated that both of the cation and anion could impact the gelation behaviors. As shown in Table 1, no gelation

**Table 1.** Influence of the Salts on the Gelation

salt	$n_{\beta\text{-CD}}$ (mmol)	$\omega_{\text{salt}}$ (%)	state <sup>a</sup>
no salt	0.88	0	S
$\text{Li}_2\text{CO}_3$	0.88	7.3	SP
$\text{Na}_2\text{CO}_3$	0.88	7.3	$\text{PG}_A$
$\text{K}_2\text{CO}_3$	0.88	7.3	DPTG
$\text{Rb}_2\text{CO}_3$	0.88	7.3	DPTG
$\text{Cs}_2\text{CO}_3$	0.88	7.3	$\text{G}_A$
$\text{KHCO}_3$	0.88	7.3	$\text{G}_A$
$\text{HCOOK}$	0.88	7.3	$\text{G}_A$
$\text{CH}_3\text{COOK}$	0.88	7.3	SP
$\text{K}_2\text{C}_2\text{O}_4$	0.88	7.3	SP
$\text{KHC}_2\text{O}_4$	0.88	7.3	SP
$\text{K}_2\text{SO}_4$	0.88	7.3	P
$\text{KClO}_3$	0.88	7.3	P
$\text{MnSO}_4$	0.88	7.3	P
$\text{MgSO}_4$	0.88	7.3	P
$\text{ZnCl}_2$	0.88	7.3	P
$\text{BaCl}_2$	0.88	7.3	P
$\text{CaCl}_2$	0.88	7.3	P

<sup>a</sup>S, solution; SP, suspension;  $\text{PG}_A$ , partial gel formed after cooling the solution; DPTG, double phase transforming gel;  $\text{G}_A$ , gel formed after cooling the solution; P, precipitate.



behavior was observed in the absence of salt. With the increase of the cationic radius of the group one element, the gelation behaviors were increasingly obvious:  $\text{Li}_2\text{CO}_3$  triggered turbid and viscous suspension,  $\text{Na}_2\text{CO}_3$  induced the system into partial gel A that the solvent was partially gelled after cooling the solution, only  $\text{K}_2\text{CO}_3$  and  $\text{Rb}_2\text{CO}_3$  could stimulate the formation of the double phase transforming gel, and  $\text{Cs}_2\text{CO}_3$  could only trigger the formation of gel A possibly due to the large size of  $\text{Cs}^+$ . After replacing  $\text{CO}_3^{2-}$  with the anions that have the similar structures, the gelation behaviors appeared in different degrees:  $\text{KHCO}_3$  and  $\text{HCOOK}$  could stimulate the system into gel A;  $\text{CH}_3\text{COOK}$ ,  $\text{K}_2\text{C}_2\text{O}_4$ , and  $\text{KHC}_2\text{O}_4$  triggered the system into the turbid and viscous suspension. Other salts that were quite different from  $\text{K}_2\text{CO}_3$  could only cause precipitates.

From the result we can infer that in order to form the gel–sol–gel' system, the radius of the cation should be between the  $\text{K}^+$  and  $\text{Rb}^+$ ;  $\text{CO}_3^{2-}$  was an irreplaceable anion. The formation of the double phase transforming gel was the inferred as the results of the delicate interactions between the cation, anion, and cyclodextrin.

**3.2.4. Effect of the Solvent on the Gelation.** Investigations of the solvent on the gelation behavior indicated that the 1,2-propylene glycol was the only solvent that could form the double phase transforming gel. As shown in Table 2, glycerin

**Table 2. Gelation Properties of  $\text{K}_2\text{CO}_3$  and  $\beta$ -CD in Various Solvents**

solvent	$n_{\beta\text{-CD}}$ (mmol)	$\omega_{\text{salt}}$ (%)	state <sup>a</sup>
glycerin	0.88	7.30	G <sub>A</sub>
ethylene glycol	0.88	7.30	S
1-propanol	0.88	7.30	P
1-butanol	0.88	7.30	P
1-pentanol	0.88	7.30	P
<i>N,N</i> -dimethylformamide	0.88	7.30	G <sub>C</sub>
<i>N,N</i> -dimethylacetamide	0.88	7.30	G <sub>C</sub>
triethylamine	0.88	7.30	P
<i>n</i> -hexane	0.88	7.30	P
trichloromethane	0.88	7.30	P
ethyl acetate	0.88	7.30	P

<sup>a</sup>G<sub>A</sub> gel formed after cooling the solution; S, solution; P, precipitate; G<sub>C</sub>, gel formed under stirring at room temperature.

could be gelled after cooling the solution. *N,N*-Dimethylformamide and *N,N*-dimethylacetamide could be gelled at room temperature. Ethylene glycol formed transparent solution while 1-propanol, 1-butanol, 1-pentanol, triethylamine, *n*-hexane, trichloromethane, and ethyl acetate caused precipitate. This result might be related to the different solubility of the gelators in different solvents and the different interactions between the solvent and  $\beta$ -CD. As  $\beta$ -CD is insoluble in 1-propanol, 1-butanol, 1-pentanol, triethylamine, *n*-hexane, trichloromethane, and ethyl acetate, the solution could not be gelled. The solubility of  $\beta$ -CD in ethylene glycol is too high, and the transparent solution was observed. As its relatively low solubility in glycerin, *N,N*-dimethylformamide and *N,N*-dimethylacetamide and appropriate interactions with the solvents, the  $\beta$ -CD resulted in gelation in these systems.

**3.2.5. Effect of the Guest on the Gelation.** As a supramolecular host,  $\beta$ -CD could include different guest molecules. The effects of adding guest molecules to the double phase transforming organogel systems were investigated. As

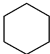
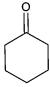
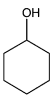
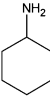
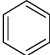
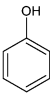
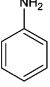
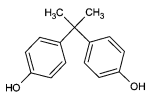
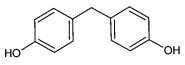
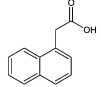
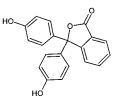
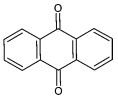
shown in Table 3, the gel–sol–gel' systems were sensitive to the guest molecules and could only remain the double phase transforming property with some specific guest molecules such as cyclohexanamine, aniline, and anthraquinone. Cyclohexanamine could stabilize both gel A and gel B by increasing the  $T_{\text{GS}}$  and decreasing the  $T_{\text{SG}}$ . In contrast, aniline could decrease the stability of gel A and stabilize gel B by decreasing  $T_{\text{GS}}$  and  $T_{\text{SG}}$ . Because of its relatively big size which could not be included in the  $\beta$ -CD-based networks, anthraquinone had no obvious effect on the gel–sol–gel' behaviors according to  $T_{\text{GS}}$  and  $T_{\text{SG}}$ . With the increase of the length of the fatty alcohol chains, the double phase transforming organogel systems turned into the stable gel systems which could be formed under the room temperature and could endure the high temperature to the boiling point of the solvent. Cyclohexane and cyclohexanone had the same effect as the long-chain fatty alcohols. This result indicated that after including these guest molecules,  $\beta$ -CD could easily aggregate into the stable network structures and irreversibly gelate the solvent. Benzene, phenol, bisphenol A, bisphenol F, 1-naphthaleneacetic acid, and phenolphthalein could turn the gel–sol–gel' systems into the gel–sol systems based on heating. This result revealed that these guest molecules could probably prevent the formation of the networks of gel B. On the contrary, cyclohexanol transformed the gel–sol–gel' system into sol–gel' system, indicating that cyclohexanol may prevent the formation of the network of gel A. The sensitivities of the gel–sol–gel' system to different guest molecules may result from the interactions between the guest molecules and  $\beta$ -CD, which is being further studied.

**3.2.6. Rheological Properties of the Gel System.** In the rheological measurement, the samples of gel A and gel B were deformed sinusoidally with frequency  $f$  to give the elastic modulus ( $G'$ ) and viscous modulus ( $G''$ ). As shown in Figure 6, the  $G'$  values of the samples were basically invariant with the frequencies, and the  $G'$  values exceeded  $G''$  values over the entire range of frequencies in samples of gel A and gel B. These results demonstrated that both of the samples were true gels.<sup>10</sup> In addition, the  $G'$  values (Figure 6b) of gel B were much larger than that (Figure 6a) of gel A, indicating that gel B exhibited a higher intensity. This result might be related to the rod-like structure of gel B which has lower elastic property.

### 3.3. Possible Mechanisms for the Gel Formation.

**3.3.1. Interactions in the Gel System Investigated by FT-IR.** The trace of the interactions between the salt and  $\beta$ -CD could be found by comparing FT-IR spectra of gel A, gel B, and physical mixture of  $\beta$ -CD and  $\text{K}_2\text{CO}_3$ . As shown in Figure 7, the absorption band of the asymmetric stretching vibration of O–H of gel A and gel B changed significantly; both of them showed a blue shift, indicating the hydrogen bond was weakened. This result might be related to the additional coordination among the  $\text{K}^+$ ,  $\text{CO}_3^{2-}$ , and the hydroxyl of  $\beta$ -CD after introducing  $\text{K}_2\text{CO}_3$  into this system, and as a result the interactions between the hydrogen and oxygen were weakened. In addition, the FT-IR spectra of gel A, gel B, and physical mixture of  $\beta$ -CD/ $\text{K}_2\text{CO}_3$  matched quite well, indicating that  $\beta$ -CD could not be converted to other compounds during the gel–sol–gel' transforming process. The same result could also be obtained by comparing the  $^1\text{H}$  NMR spectra (Figure S1) of xerogel A, xerogel B, and native  $\beta$ -CD. From the results mentioned above, we can infer that the gel–sol–gel' transforming process may be related to the interactions between  $\beta$ -CD and  $\text{K}_2\text{CO}_3$ .

Table 3. Influence of the Guest on the Double Phase Transforming Gel Systems<sup>a</sup>

guest molecular(0.11 mol•L <sup>-1</sup> )	molecular formula	phase behavior	T <sub>GS</sub> /°C	T <sub>SG</sub> /°C
no guest		gel-sol-gel'	72	117
1-hexanol	CH <sub>3</sub> (CH <sub>2</sub> ) <sub>5</sub> OH	gel-sol-gel'	56	114
dodecanol	CH <sub>3</sub> (CH <sub>2</sub> ) <sub>11</sub> OH	gel		
stearyl alcohol	CH <sub>3</sub> (CH <sub>2</sub> ) <sub>17</sub> OH	gel		
cyclohexane		gel		
cyclohexanone		gel		
cyclohexanol		sol-gel'		104
cyclohexanamine		gel-sol-gel'	81	104
benzene		gel-sol	67	
phenol		gel-sol	68	
aniline		gel-sol-gel'	69	108
bisphenol A		gel-sol	105	
bisphenol F		gel-sol	65	
1-naphthaleneacetic acid		gel-sol	58	
phenolphthalein		gel-sol	73	
anthraquinone		gel-sol-gel'	71	116

<sup>a</sup>c<sub>β-CD</sub> = 0.11 mol L<sup>-1</sup>, ω<sub>K<sub>2</sub>CO<sub>3</sub></sub> = 3.9%.

3.3.2. Structure Investigation by Small-Angle XRD. XRD could be employed to provide an insight into the crystal

structure of β-CD which could be generally classified into two types: cage type and channel type.<sup>27</sup> Figure 8 shows the XRD

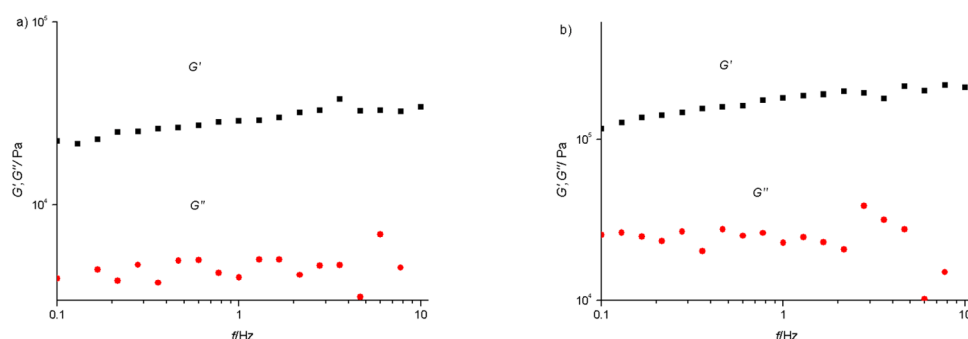


**Figure 6.** Rheological properties of gel A (a) and gel B (b) ( $c_{\beta\text{-CD}} = 0.18 \text{ mol L}^{-1}$ ,  $\omega_{\text{K}_2\text{CO}_3} = 7.3\%$ ,  $\text{K}_2\text{CO}_3/1,2\text{-propylene glycol}$ , w/w).

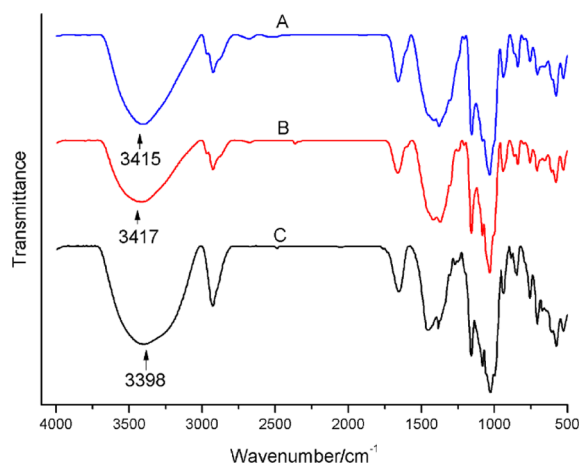


**Figure 7.** FT-IR spectra of xerogel A (A), xerogel B (B), and physical mixture of  $\beta\text{-CD}/\text{K}_2\text{CO}_3$  (C) ( $c_{\beta\text{-CD}} = 0.18 \text{ mol L}^{-1}$ ,  $\omega_{\text{K}_2\text{CO}_3} = 7.3\%$ ,  $\text{K}_2\text{CO}_3/1,2\text{-propylene glycol}$ , w/w).

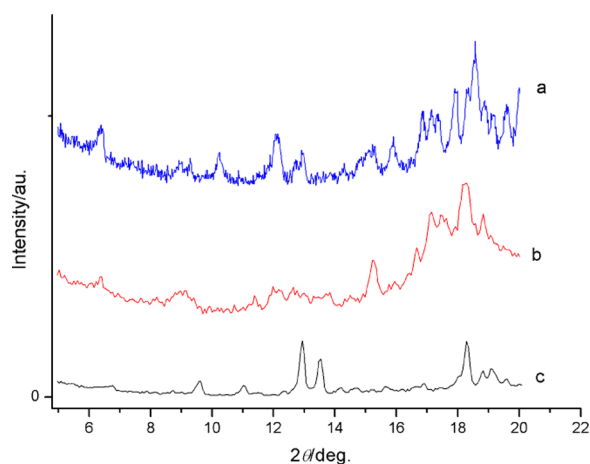


**Figure 8.** Small-angle XRD spectra of xerogel of gel A (a), xerogel of gel B (b), and physical mixture of  $\beta\text{-CD}$  and  $\text{K}_2\text{CO}_3$  (c) ( $c_{\beta\text{-CD}} = 0.18 \text{ mol L}^{-1}$ ,  $\omega_{\text{K}_2\text{CO}_3} = 7.3\%$ ,  $\text{K}_2\text{CO}_3/1,2\text{-propylene glycol}$ , w/w).

patterns of xerogel A, xerogel B, and physical mixture of  $\beta\text{-CD}$  and  $\text{K}_2\text{CO}_3$ . In Figure 8c, major peaks at  $9.5^\circ$ ,  $12.9^\circ$ ,  $13.4^\circ$ , and  $18.2^\circ$  were observed, indicating the  $\beta\text{-CD}$  molecules were arranged in cage-type structure.<sup>28</sup> However, XRD patterns of xerogel A were quite different from that of the physical mixture. Main signals at  $2\theta = 12.7^\circ$  ( $d = 0.70 \text{ nm}$ , the depth of the  $\beta\text{-CD}$  cavity) and  $2\theta = 6.3^\circ$  ( $d = 1.40 \text{ nm}$ , 2 times the depth of the  $\beta\text{-CD}$  cavity) are the characteristic peaks of head-to-head channel

type  $\beta\text{-CD}$  assemblies, suggesting the  $\beta\text{-CD}$  were arranged by head-to-head channel type structure.<sup>29,30</sup> The xerogel B appeared to be less crystalline than xerogel A, but the XRD pattern of xerogel B matched quite well with that of xerogel A especially at the peaks of  $12.7^\circ$  and  $6.3^\circ$ , indicating the presence of channel type  $\beta\text{-CD}$  assemblies.

According to the SEM observations and rheological data, the xerogel B was composed of nanorods and exhibited higher intensity; we speculate that the length of channel type  $\beta\text{-CD}$  assemblies was much longer so that they could grow toward one direction and form the nanorods. On the contrary, the shorter channel type  $\beta\text{-CD}$  could grow isotropously and exhibit the nanospheres structure.

According to the combination of the results mentioned above, we proposed a possible model (Scheme 1) of the formations of three-dimensional networks of gel A and gel B. In the model, the dispersed  $\beta\text{-CD}$  aggregate into nanospheres which are composed of shorter channel-type assemblies of  $\beta\text{-CD}$  with the help the  $\text{K}^+$  and  $\text{CO}_3^{2-}$  after cooling the solution. The nanospheres aggregate further into three-dimensional network. Because of the huge interface tension of the network, the solvent is gelated and gel A is obtained; the dispersed  $\beta\text{-CD}$  aggregate into nanorods which are composed of longer channel-type assembly of  $\beta\text{-CD}$  with the help the  $\text{K}^+$  and  $\text{CO}_3^{2-}$  after heating the solution. The nanorods interlace with each other, and the capillary forces are formed. The solvent is immobilized by the capillary forces, and gel B is observed.

In order to test and verify the possibility of the model proposed in Scheme 1, the dynamic simulations of gel A and gel B were performed with the software Material Studio 4.3 by Accelrys.<sup>23</sup> After finishing the simulation, two images (Figure S2) of the gelation systems were obtained, and the molecules of the solvent were deleted in order to view the structures of the  $\beta\text{-CD}$  assemblies clearly. Figure 9a exhibited the shorter channel type assemblies of  $\beta\text{-CD}$  while Figure 9b was the longer channel type assemblies of  $\beta\text{-CD}$ . The gaps between different  $\beta\text{-CD}$  were filled with  $\text{K}^+$  and  $\text{CO}_3^{2-}$  which play the roles of associating different  $\beta\text{-CD}$  by electrostatic attractions. The results were in consistency with the model we proposed in Scheme 1.

#### 4. CONCLUSIONS

In conclusion, we have achieved a novel double phase transforming organogel by employing  $\beta\text{-CD}$ ,  $\text{K}_2\text{CO}_3$ , and 1,2-propylene glycol. The transforming processes are accompanied by a reversible gel–sol transforming process and an irreversible sol–gel transforming process based on heating. The formations of the gel and gel' are presumed to be related to the constructions of three-dimensional networks of nano-

Scheme 1. Schematic Illustration of the Formation of Three-Dimensional Networks of Nanospheres and Nanorods

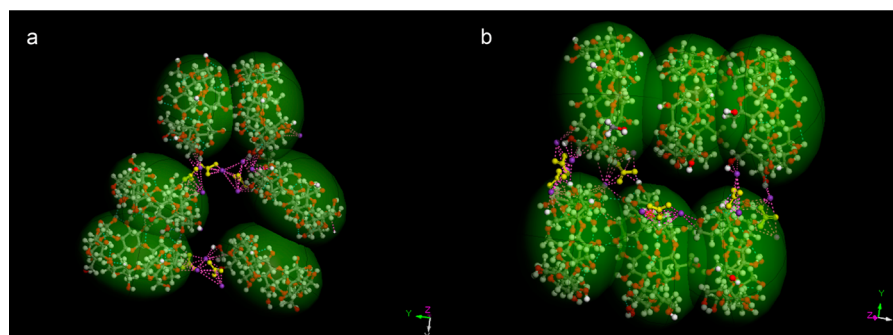
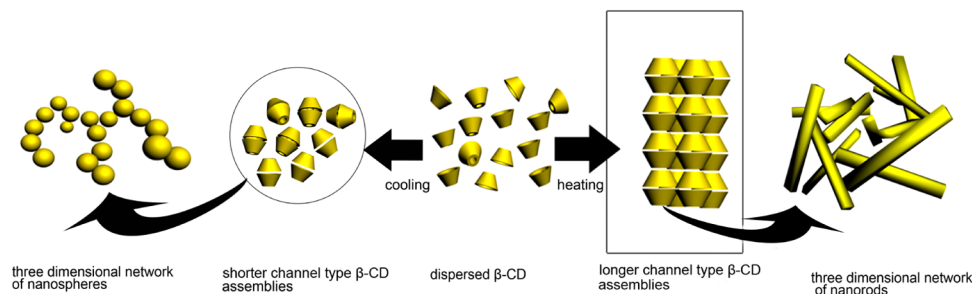


**Figure 9.** Possible gelation model of the gel structures (green ellipsoid,  $\beta$ -CD; yellow molecule,  $\text{CO}_3^{2-}$ ; purple ball,  $\text{K}^+$ ): (a) shorter channel type  $\beta$ -CD assemblies,  $T = 298 \text{ K}$ ; (b) longer channel type  $\beta$ -CD assemblies,  $T = 393 \text{ K}$ .

spheres and nanorods, respectively, which immobilize the solvent through surface tension and capillary forces.  $\text{K}_2\text{CO}_3$  plays a key role in associating supramolecular architectures of  $\beta$ -CD. This novel double phase transforming system could have potential applications in smart materials, drug-delivery systems, biomaterials, and other fields.

## ■ ASSOCIATED CONTENT

### ● Supporting Information

$^1\text{H}$  NMR spectra of xerogel A, xerogel B, and physical mixture; possible gelation model of the gel structures by the dynamic simulations. This material is available free of charge via the Internet at <http://pubs.acs.org>.

## ■ AUTHOR INFORMATION

### Corresponding Author

\*Tel +86-531-88363306; Fax +86-531-88564464; e-mail [haoay@sdu.edu.cn](mailto:haoay@sdu.edu.cn).

### Notes

The authors declare no competing financial interest.

## ■ ACKNOWLEDGMENTS

This work was supported by the NSFC (Grant No. 20625307) and National Basic Research Program of China (973 Program, 2009CB930103). We gratefully thank Pro. Yuxiang Bu, Professor Shiling Yuan, Dr. Jinxiang Liu, and Dr. Hua Wang from the Center of Molecular Modeling & Simulation, Institutes of Theoretical Chemistry, Shandong University, for the help with dynamic simulations.

## ■ REFERENCES

- (1) Burnworth, M.; Tang, L.; Kumpfer, J. R.; Duncan, A. J.; Beyer, F. L.; Fiore, G. L.; Rowan, S. J.; Weder, C. *Nature* **2011**, *472*, 334–337.
- (2) Huck, W. T. S. *Nature* **2011**, *472*, 425–426.

- (3) Kim, J.; Hanna, J. A.; Byun, M.; Santangelo, C. D.; Hayward, R. C. *Science* **2012**, *335*, 1201–1205.
- (4) Sieradzki, K. *Science* **2011**, *332*, 1158–1159.
- (5) Vintiloiu, A.; Leroux, J.-C. *J. Controlled Release* **2008**, *125*, 179–192.
- (6) Wang, K.; Jia, Q.; Yuan, J.; Li, S. *Int. J. Pharm.* **2011**, *404*, 176–179.
- (7) Llusar, M.; Sanchez, C. *Chem. Mater.* **2008**, *20*, 782–820.
- (8) Puigmartí-Luis, J.; Laukhin, V.; Pérez del Pino, Á.; Vidal-Gancedo, J.; Rovira, C.; Laukhina, E.; Amabilino, D. B. *Angew. Chem., Int. Ed.* **2007**, *46*, 238–241.
- (9) Teng, M.; Kuang, G.; Jia, X.; Gao, M.; Li, Y.; Wei, Y. *J. Mater. Chem.* **2009**, *19*, 5648–5654.
- (10) Piepenbrock, M.-O. M.; Lloyd, G. O.; Clarke, N.; Steed, J. W. *Chem. Rev.* **2010**, *110*, 1960–2004.
- (11) Sangeetha, N. M.; Maitra, U. *Chem. Soc. Rev.* **2005**, *34*, 821–836.
- (12) Wilder, E. A.; Wilson, K. S.; Quinn, J. B.; Skrtic, D.; Antonucci, J. M. *Chem. Mater.* **2005**, *17*, 2946–2952.
- (13) Fages, F. *Angew. Chem., Int. Ed.* **2006**, *45*, 1680–1682.
- (14) Foster, J. A.; Steed, J. W. *Angew. Chem., Int. Ed.* **2010**, *49*, 6718–6724.
- (15) Mohmeyer, N.; Schmidt, H. W. *Chem.—Eur. J.* **2005**, *11*, 863–872.
- (16) Adhikari, B.; Nanda, J.; Banerjee, A. *Chem.—Eur. J.* **2011**, *17*, 11488–11496.
- (17) Zhao, W.; Li, Y.; Sun, T.; Yan, H.; Hao, A.; Xin, F.; Zhang, H.; An, W.; Kong, L.; Li, Y. *Colloids Surf., A* **2011**, *374*, 115–120.
- (18) Wang, C.; Li, Z.; Wang, X.; Wei, W.; Chen, S.; Sui, Z. *Colloids Surf., A* **2011**, *384*, 490–495.
- (19) Kida, T.; Marui, Y.; Miyawaki, K.; Kato, E.; Akashi, M. *Chem. Commun.* **2009**, 3889–3891.
- (20) Marui, Y.; Kikuzawa, A.; Kida, T.; Akashi, M. *Langmuir* **2010**, *26*, 11441–11445.
- (21) Wang, D.; Hao, J. C. *Langmuir* **2011**, *27*, 1713–1717.
- (22) Wang, C.; Chen, Q.; Sun, F.; Zhang, D.; Zhang, G.; Huang, Y.; Zhao, R.; Zhu, D. *J. Am. Chem. Soc.* **2010**, *132*, 3092–3096.

- (23) Li, Y.; Liu, J.; Du, G.; Yan, H.; Wang, H.; Zhang, H.; An, W.; Zhao, W.; Sun, T.; Xin, F.; et al. *J. Phys. Chem. B* **2010**, *114*, 10321–10326.
- (24) Yamanaka, M.; Fujii, H. *J. Org. Chem.* **2009**, *74*, 5390–5394.
- (25) Frkanec, L.; Jokic, M.; Makarevic, J.; Wolsperger, K.; Zinic, M. *J. Am. Chem. Soc.* **2002**, *124*, 9716–9717.
- (26) van Esch, J. H.; Feringa, B. L. *Angew. Chem., Int. Ed.* **2000**, *39*, 2263–2266.
- (27) Saenger, W.; Jacob, J.; Gessler, K.; Steiner, T.; Hoffmann, D.; Sanbe, H.; Koizumi, K.; Smith, S. M.; Takaha, T. *Chem. Rev.* **1998**, *98*, 1787–1802.
- (28) Gao, Y. a.; Zhao, X.; Dong, B.; Zheng, L.; Li, N.; Zhang, S. *J. Phys. Chem. B* **2006**, *110*, 8576–8581.
- (29) Kong, L.; Sun, T.; Xin, F.; Zhao, W.; Zhang, H.; Li, Z.; Li, Y.; Hou, Y.; Li, S.; Hao, A. *Colloids Surf., A* **2011**, *392*, 156–162.
- (30) Liu, L.; Zhu, S. *Carbohydr. Polym.* **2007**, *68*, 472–476.